A novel technique to detect a fault during a power swing using pilot relaying

Hesham B. Elrefaie
Electrical Engg. Dept., Faculty of Engg., Alexandria University, Alexandria, Egypt
E-mail: hasham.elrefai@hotmail.com

This paper describes a technique to detect a fault during a power swing using pilot relaying. This technique is based on calculating the reactive power at the sending end and receiving ends busbars using the instantaneous values of the three phase voltage signals and the three phase current signals measured at both ends. The average values of the reactive powers are calculated at both ends of the protected line. The internal fault can be detected if the average value of the reactive power at one end is increasing and that one at the other end is decreasing. The external fault can be detected if the average values of the reactive power at both ends are increasing. This technique can detect all fault types and can distinguish between internal and external fault. The Alternative Transient Program (ATP) is used in this paper to simulate the fault types and power swing and the Matlab software package is used to estimate the reactive power and its average value.

تصف هذة المقالة تقنية جديدة لكشف الأخطاء أثناء تأرجحات القوى باستخدام مرحل اختبار. تعتمد هذة التقنية على حساب القدرة الغير فعالة عند قضبان الإرسال و عند قضبان الاستقبال باستخدام القيم اللحظية لموجات الجهد و التيار المقاسة عند هذه القضبان. وتم حساب القيم المتوسطة للقدرات الفعالة عند هذه القضبان. ويمكن تحديد الأخطاء الداخلية لخط النقل الكهربي إذا زادت القيمة المتوسطة للقدرة الغير فعالة عند أحدى القضبان فجأة وانخفضت القيمة المتوسطة للقدرة الغير فعالة عند القضيب الأخر. ويمكن تحديد الأخطاء الخارجية لخط النقل الكهربي إذا زادت القيم المتوسطة للقدرة الغير فعالة فجأة عند قضبان الإرسال و الاستقبال. ويمكن لهذه التقنية تحديد الأخطاء المختلفة والتفرقة بين الأخطاء الداخلية و الخارجية. واستخدم برنامج الحالات العابرة البديل في تمثيل الأخطاء المختلفة و تأرجحات القوى واستخدم برنامج ماتلاب في حساب القدرة الغير الفعالة والقيم المتوسطة لها.

Keywords: Digital protection of power systems, Distance relays, Power swing

1. Introduction

Power swings are oscillations in power flow, which might be caused by sudden removal of faults, loss of synchronism or changes in direction of power flow as a result of switching. A power swing may cause the appearance impedance measured by a distance relay to move away from the normal load area and into one or more of its tripping characteristics, and thus causes unwanted trip. To ensure the stability of distance relay, a power swing blocking functions is integrated in most of modern distance relays to block the operation during pure power swing [1]. On the other hand, after a fault occurs during the power swing, the distance relay should be able to detect the fault and trip the internal fault as soon as possible.

Several schemes are proposed to detect a permanent fault during the power swing. Benmouyal et al. [2] track the Swing Center Voltage (SCV) defined as "the voltage at the location of a two-source equivalent system, where the voltage value is zero when the angles between the two sources are 180 apart". Mechraoui and Thomas [3] consider the changing frequency in their formulation, build a model in time invariant (d-q) frame and track the load angle to differentiate between a swing and a fault. Brahma [4] introduces the use of the Wavelet Transform (WT) to detect a power swing and to detect a symmetrical fault during a power swing. Lin et al. [5] propose an unblocking scheme for the distance protection based on the variation rates of both active and reactive power to identify symmetrical faults occurring during power swing.

This paper describes a technique to detect a fault during a power swing. This technique is based on comparing the average values of the reactive powers estimated at both sending and receiving end busbars.

© Faculty of Engineering, Alexandria University, Egypt.

2. System under study

Fig.1 shows the system selected for simulation. The system details are given in the Appendix and ref. [6]. This system has been extensively used by industry professionals [1] and researchers [3-4]. The system is simulated using the Alternative Transient Program (ATP) [7]. The system consists of a 830 MVA turbo generator supplying power to an infinite bus over a transformer, a 72 km long double circuit transmission line (L1 and L2), and a 72 km long single circuit transmission line (L3). The pilot relays are located at breakers B1 and B2. A disturbance is created by a three phase fault at location F2 (the middle of L2) after 0.1 second from the simulation starting instant. This fault is cleared after a time interval of 0.05 second by disconnecting the faulted line at BUS 1 and BUS 2 (breakers B3 and B4). Such disturbance on the power system will cause the generator to accelerate or decelerate resulting in a power swing, in severe cases, a pole slip. Fig. 2 and fig. 3 show the voltage and current waveforms observed at busbar 1. Figs. 4 and 5 show the voltage and current waveforms observed at busbar2. The prefault load angle (δ), used in simulating these waveforms, is 30° (the angle between the turbo generator equivalent voltage source and the infinite busabar equivalent voltage source). It is noted from these figures, during the power swing, when the voltages are maximum currents are minimum and when currents are at peak voltages are close to zero. This note agrees with that mentioned about the voltage and current waveforms shown in refs. [4 - 5]. The waveforms shown in figures are also similar to those given in refs. [4 - 5].

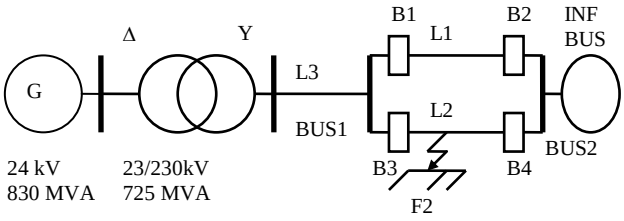

Fig. 1. System under study.

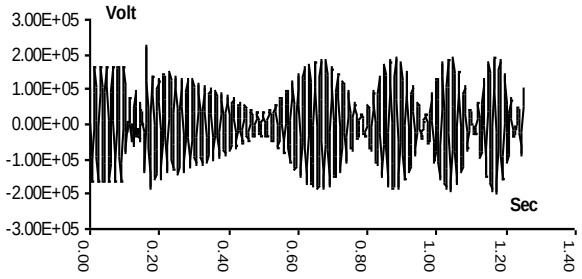

Fig. 2. The voltage signal of phase a observed at BUS1 during the power swing.

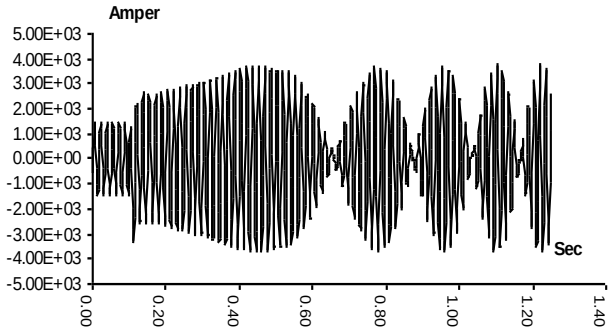

Fig. 3. The current signal of phase a observed at BUS1 during the power swing.

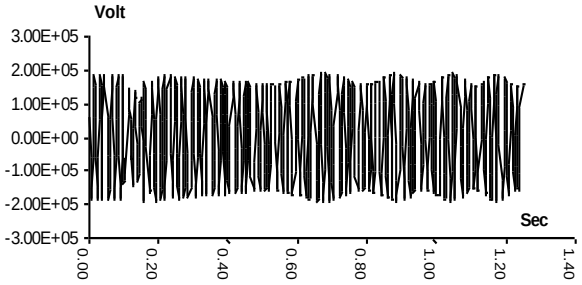

Fig. 4. The voltage signal of phase a observed at BUS2 during the power swing.

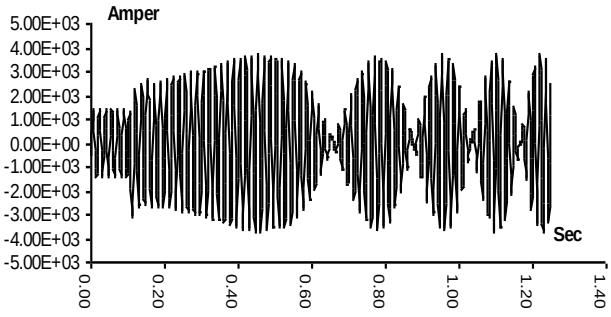

Fig. 5. The current signal of phase a observed at BUS2 during the power swing.

3. Reactive power calculating algorithm

The general reactive power calculating algorithm usually utilizes the vectors of voltage and current resulting from the Discrete Fourier Transform (DFT). If the DFT is utilized, it must make sure that the total time intervals of all involved sampling values consists of a complete power frequency cycle. Otherwise remarkable calculation error is inevitable. Frequency tracking should be used to ensure full periodic sampling. However, it is very difficult to be guaranteed during power swings. Therefore, we prefer to utilize a power algorithm immune to time-varied frequency. In this paper, an algorithm based on instantaneous measurement of voltages and currents is selected [5]:

$$Q_i = \frac{1}{\sqrt{3}}[u_{ai}(i_{ci} - i_{bi}) + u_{bi}(i_{ai} - i_{ci}) + u_{ci}(i_{bi} - i_{ai}), \quad (1)$$

where, u_{ai}, u_{bi}, u_{ci} and i_{ai}, i_{bi}, i_{ci} are the latest instantaneous phase voltages and phase currents. Fixed sampling rate (e.g. 1.2 k Hz) can be used to perform the sampling task. In this case, the calculation of Q will not be affected by the change of system frequency.

In order to eliminate the effect of high harmonics, we can evaluate the average reactive power cycle at each sampling point as follows:

$$Q_a = \frac{1}{N_s} \sum_{i=m-N_s+1}^{m} Q_i \ , \quad (2)$$

where m is the subscript of the latest sampling and N_s is the length of a time window in the case of a fixed sampling rate, for instance, 20 for a 1.2 k Hz sampling rate.

Fig. 6 shows the reactive powers Q_r and Q_s calculated at receiving end, BUS1, and sending end, BUS2, respectively. As seen from this figure, both Q_r and Q_s appear as sine waveforms whose amplitudes are nearly steady. The Matlab software package [8] is used to calculate the reactive powers.

4. A fault occurring during the power swing

Eight cases are studied by simulating different fault types during the power swing. In all cases the fault occurs after one second from the simulation starting instant. The first case is studied by simulating a three line to ground fault on the middle of the line L1 (internal fault). Fig. 7 shows the reactive powers Q_r and Q_s calculated at the receiving end, BUS1, and the sending end, BUS2, respectively. As seen from this figure a rise in the value of Q_s and a reduction in the value of Q_r are observed after the fault occurrence. It is noted also from the figure, that both Q_s and Q_r appear as straight lines after the fault occurrence. The second case is studied by simulating a three line to ground fault on the middle of the line L3. In this case, a rise in the value of Q_r is observed after the fault occurrence as shown in fig. 8. Also, both Q_s and Q_r appear as straight lines after the fault occurrence. The third case is studied by simulating a single line to ground fault on the middle of the line L1. In this case, a rise in the value of Q_s and a reduction in the value of Q_r are observed after the fault occurrence as shown in fig. 9. Both Q_s and Q_r appear as sine waveforms after the fault occurrence with amplitudes different than those observed during the power swing. The fourth case is studied by simulating a single line to ground fault on the middle of the line L3. In this case, a rise in Q_r is observed after the fault occurrence as shown in fig. 10. Also, both Q_s and Q_r appear as sine waveforms after the fault occurrence with amplitudes different than those observed during the power swing. The fifth case is studied by simulating a double line to ground fault on the middle of the line L1. In this case, a rise in the value of Q_s and a reduction in the value of Q_r are observed after the fault occurrence as shown in fig. 11. The amplitudes of Q_s and Q_r after the fault occurrence are different than those observed during the power swing and smaller than those observed after the occurrence of the single line to ground fault. The sixth case is studied by simulating a double line to ground fault on the middle of the line L3. In this case, a rise in the value of Q_r is observed after the fault occurrence as shown in fig. 12.

Also, the amplitudes of Q_s and Q_r after the fault occurrence are more different from those observed during the power swing and smaller than those observed after the occurrence of the single line to ground fault. The seventh case is studied by simulating a double line fault on the middle of the line L1. In this case a rise in Q_s and a reduction in Q_r are observed after the fault occurrence as shown in fig. 13. The amplitudes of Q_s and Q_r after the fault occurrence are different from those observed during the power swing, smaller than those observed after the occurrence of the single line to ground fault, and similar to those observed after the occurrence of the double line to ground fault. The eighth case is studied by simulating a double line fault on the middle of the line L3. In this case, a rise in the value of Q_r is observed after the fault occurrence as shown in fig. 14. Also, the amplitudes of Q_s and Q_r are different from those observed during the power swing, smaller than those observed after the single line to ground fault occurrence, similar to those observed after the double line fault occurrence.

It is possible to conclude from the shown figures when a rise in the value of Q_s and a reduction in the value of Q_r are observed, the internal fault occurs and when both Q_s and Q_r are rising, the external fault occurs.

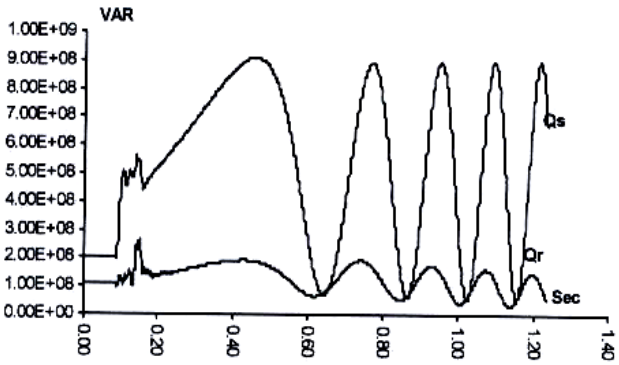

Fig. 6. The three phase reactive powers calculated at BUS1 (Q_r) and BUS2 (Q_s) during the power swing.

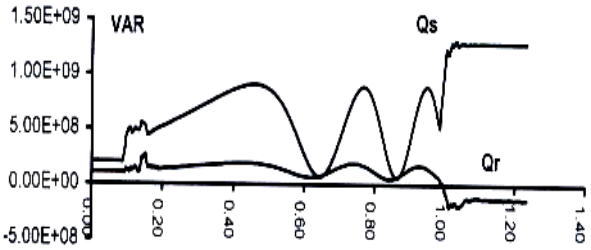

Fig. 7. The reactive powers Q_s and Q_r for three line to ground fault occurring at 50% of L1.

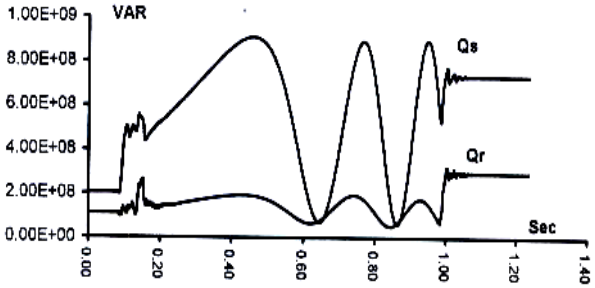

Fig. 8. The reactive powers Q_s and Q_r for three line to ground fault occurring at 50% of L3.

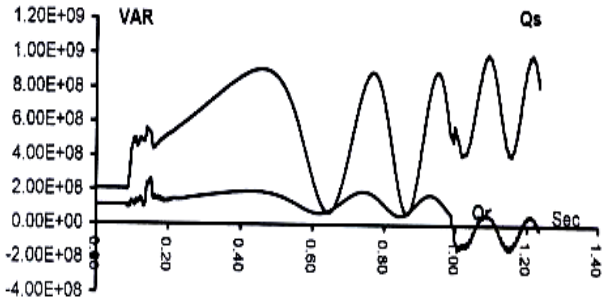

Fig. 9. The reactive powers Q_s and Q_r for single line to ground fault occurrring at 50 %of L1.

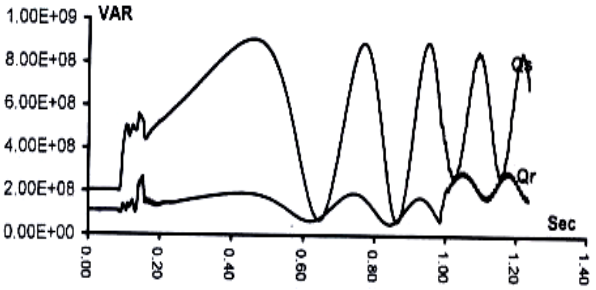

Fig. 10. The reactive powers Q_s and Q_r for single line to ground fault occurring at 50 %of L3.

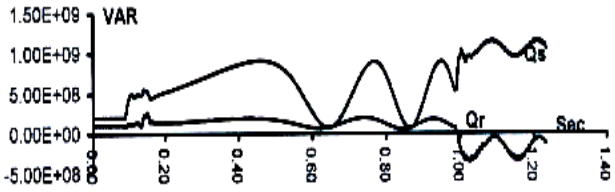

Fig. 11. The reactive powers Q_s and Q_r for double line to ground fault occurring at 50 % of L1.

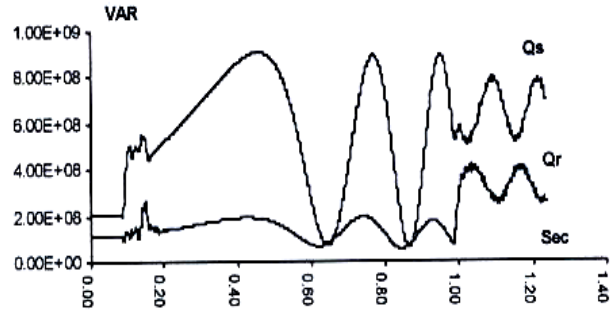

Fig. 12. The reactive powers Q_s and Q_r for double line to ground fault occurring at 50% of L3.

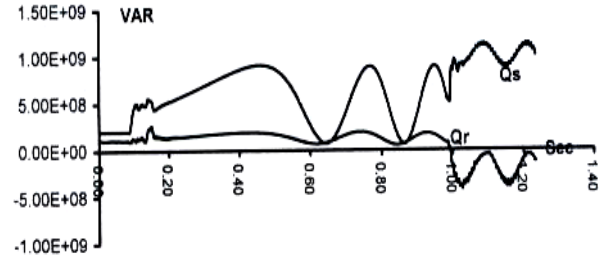

Fig. 13. The reactive powers Q_s and Q_r for double line fault occurring at 50% of L1.

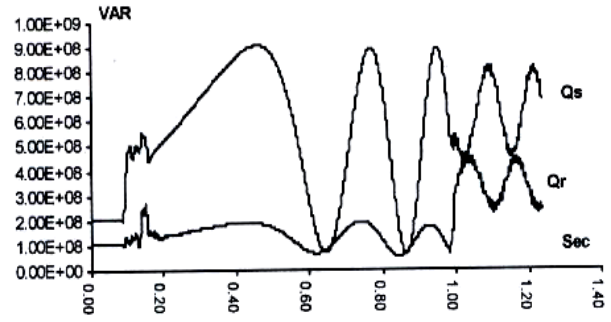

Fig. 14. The reactive powers Q_s and Q_r for double line fault at occurring 50% of L3.

5. The average value of the reactive power calculating algorithm

The reactive powers Q_s and Q_r appear as sine waveforms during the power swing, whose amplitudes are nearly steady. Each waveform has a minimum value and a maximum value. The average value is started by summing the points between the first maximum value and the first minimum value and then dividing the sum by the number of points between the maximum value and the minimum value. The average value of the reactive power can be calculated at each sampling point following the first maximum value as follows:

$$Q_{av} = \frac{1}{N_d} \sum_{i=m-N_d+1}^{m} Q_{ai} \ , \qquad (3)$$

where m is the subscript of the latest sampling and N_d is the length of a time window (N_d is 218 points for the sine waveforms Q_s and Q_r shown in fig. 6). The average values of the reactive powers shown in fig. 7 – 14 are calculated as shown in fig. 15 – 22. As seen from these figures, the values of Q_{as} and Q_{ar} are constant during the power swing then a sudden rise in the value of Q_{as} and a sudden drop in the value of Q_{ar} after the internal fault occurrence. Also, the values of Q_{as} and Q_{ar} are rising after the external fault occurrence.

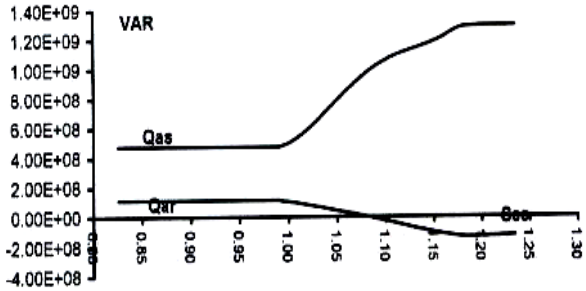

Fig. 15. The average values of Q_s and Q_r for three line to ground fault occurring at 50% of L1.

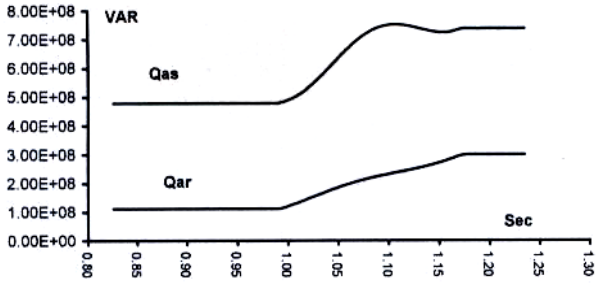

Fig. 16. The average values of *Qs* and *Qr* for three line to ground fault occurring at 50% of L3.

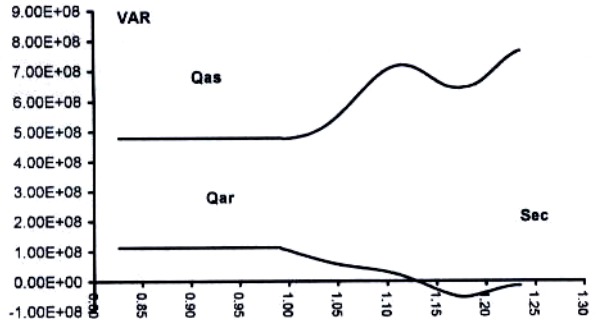

Fig. 17. The average values of *Qs* and *Qr* for single line to ground fault occurring at 50% of L1.

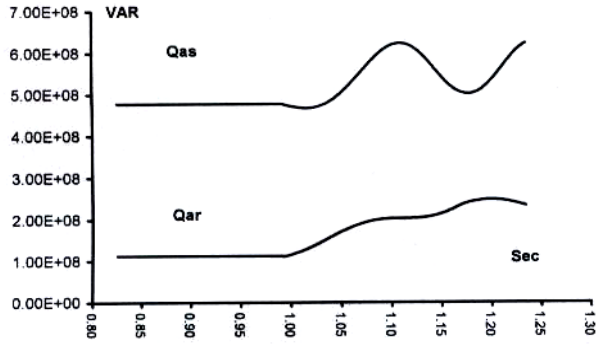

Fig. 18. The average values of *Qs* and *Qr* for single line to ground fault occurring at 50% of L3.

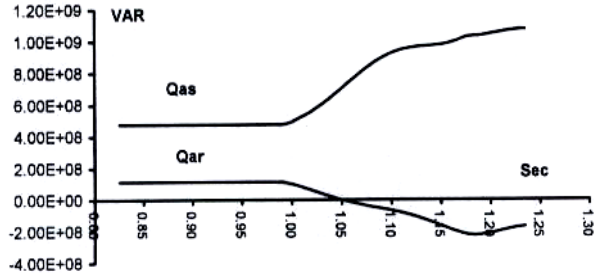

Fig. 19. The average values of *Qs* and *Qr* for double line to ground fault occurring at 50 of L1.

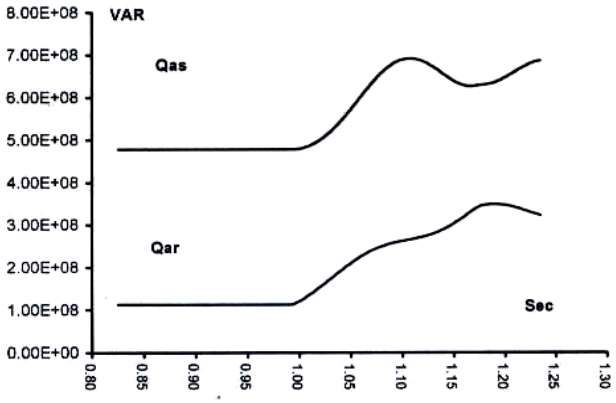

Fig. 20. The average values of *Qs* and *Qr* for double line to ground fault occurring at 50% of L3.

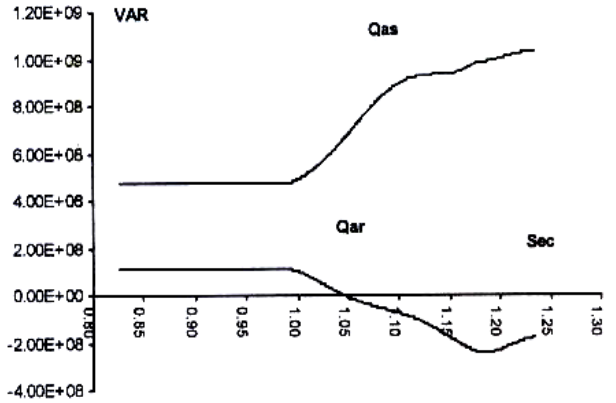

Fig. 21. The average values of *Qs* and *Qr* for double line fault occurring at 50% of L1.

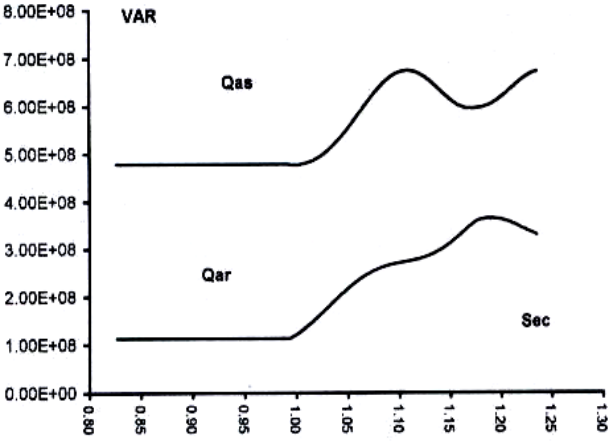

Fig. 22. The average values of *Qs* and *Qr* for double line fault occurring at 50% of L3.

6. An algorithm to detect a fault during the power swing

An algorithm to detect a fault during the power swing is proposed in this section. As seen from the shown figures, the reactive powers Q_s and Q_r are constant during the normal operation. But during the power swing, the reactive powers Q_s and Q_r appear as sine waves with constant amplitudes. Therefore, it is possible to distinguish the normal operation from the power swing by calculating $\frac{dQ_S}{dt}$ and $\frac{dQ_r}{dt}$. If these values are not zero, then the power swing is detected. Once the power swing is detected, the average values of Q_s (Q_{as}) and Q_r (Q_{ar}) are calculated. If Q_{as} are suddenly increasing and Q_{ar} is suddenly decreasing (Q_{as} and Q_{ar} are constant during the power swing), an internal fault occurs. If both Q_{as} and Q_{ar} are increasing, an external fault occurs. In the case of internal fault, a counter is started. If the value of the counter reaches 10 (half cycle), a trip command is given to isolate the circuit breakers at BUS1 and BUS2. The flow chart shown in fig. 23 explains the procedure of the suggested algorithm.

7. Comparative study

Our study is compared with refs. [4 - 5]. The following remarks can be observed.

1. Our technique can detect different fault types but the techniques suggested in refs. [4 - 5] can detect only a symmetrical fault.
2. Our technique can distinguish between internal and external fault but the techniques suggested in refs. [4 - 5] can not.
3. The voltage and current measurements at both line ends does not need to be synchronized when using our technique. Therefore our suggested technique eliminates the problem of sampling misalignment associated with digital feeder protection based on current differential as shown in ref. [9].

Based on above remarks, our suggested technique can improve the fault detection process compared with refs. [4 - 5].

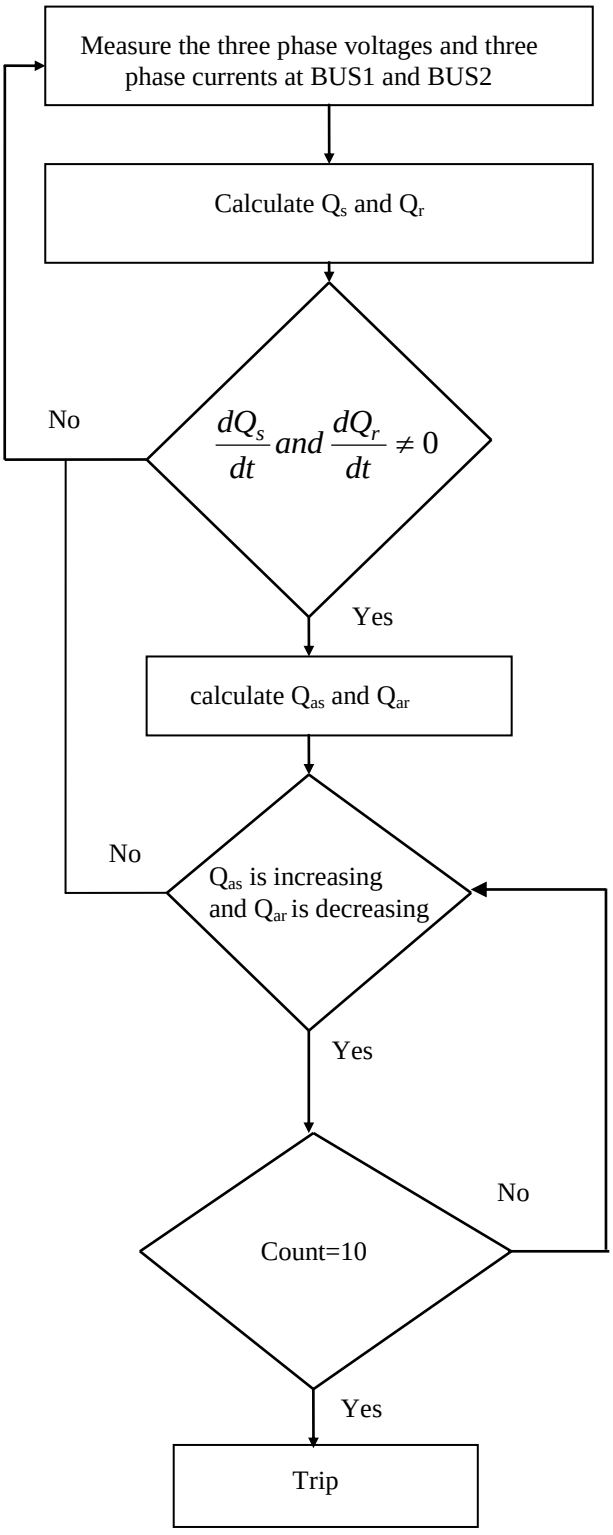

Fig. 23. The flow chart of the suggested algorithm.

8. Conclusions

This paper proposes a technique to detect a fault during the power swing. In this technique, reactive powers at sending and receiving ends are calculated using the voltage and current waveforms measured at those ends. Also, the average values of the reactive powers are calculated. The internal fault can be detected if the average value of the reactive power is suddenly increasing at one end and the average value of the reactive power is suddenly decreasing at the other end. The external fault can be detected if the average values of the reactive powers are suddenly increasing. Our technique can improve the fault detection process compared with other techniques [4 and 5] as shown in this study.

Appendix

System parameters

A.1. Infinite bus (230kV)

Positive-sequence impedance Z_1: 6.1+j 5.5 Ω
Zero-sequence impedance Z_0: 2.7+j 6.97Ω

A.2. Synchronous machine

Rated kV: 24 kV
Rated MVA: 830MVA
Armature dc resistance Ra: 0.00166Ω
Positive-sequence reactance X1 0.125 pu
Zero-sequence reactance X0 0.1208 pu
Direct-axis synchronous reactance Xd: 1.57 pu
Quadrature-axis synchronous reactance Xq:1.5pu
Direct-axis transient reactance X'd: 0.19pu
Quadrature-axis transient reactance X'q: 0.3625pu
Direct-axis sub-transient reactance X"d: 0.1479pu
Quadrature-axis sub-transient reactance X"q: 0.1475pu
Direct-axis transient open-circuit time constant T'do 4.2s
Quadrature-axis transient open-circuit time constant T'qo 0.589s
Direct-axis sub-transient open-circuit time constant T"do 0.031s
Quadrature-axis sub-transient open-circuit time constant T"qo 0.063s
Inertia constant 2.4 MW/MVA
All per-unit impedance values are on the machine base (830 MVA, 24 kV).
Exciter and governor dynamics are not modeled.

A.3. Transformer

H.V. Winding
Voltage: 229.89 kV
MVA: 725MVA
Resistance: 0.1469Ω

L.V. Winding:
Voltage: 22.8 kV
MVA: 725MVA
Resistance 0.0044Ω

%Excitation current at 100% rated voltage: 0.706
No load losses at 100% rated voltage 466.303 kW

Short-circuit Test

229.893kV to 22.8kV @ 725 MVA:

%Z: 7.67
Losses 1333.689kW

Zero-sequence quantities are assumed to be the same as positive-sequence quantities.

A.4. 230kV Transmission Lines

There are two 230kV transmission lines in the model system of fig. 1. The first is a double-circuit line and the second is a single circuit line. Each line is 72 km long, and there are three sections per line, each section is 24 km in length. The double-circuit line is modeled using a constant parameter line model and the single circuit line is modeled as lumped parameter sections. The line conductor is a Marigold 5.639 cm^2 AA with a 3.088 cm diameter and a dc resistance of 0.5763Ω/m at 50°C. The line parameters are calculated at 50 Hz with an earth resistivity of 50Ω-m.

Table 1
Tower configuration for 230 kV double-circuit line

Conductor	Horizontal separation from Reference (m)	Height at tower (m)	Height at mid span(m)
1	0.0	30.48	22.2504
2	0.0	25.45	17.2212
3	0.0	20.4216	12.19
4	8.84	20.4216	12.19
5	8.84	25.45	17.2212
6	8.84	30.48	22.2504

Table 2
Tower configuration for 230 kV single-circuit line

Conductor	Horizontal separation from reference (m)	Height at tower (m)	Height at mid span(m)
1	0.0	30.48	22.2504
2	0.0	25.45	17.22
3	0.0	20.42	12.19

References

[1] A. Apostolov, G. Benmouyal and G. Brunello, "Power Swing and Out-of-Step Considerations on Transmission Lines", [Online]. Available:http:www.pes-psrc.org.

[2] G. Benmouyal, D. Hou and D. Triouvaras, Zero-setting power-swing Blocking Protection [Online]. Available http://www.selinc.com/tech-pprs/6163.pdf.

[3] A. Mechraoui and D.W.P Thomas, "A New Blocking Principle with Phase and Earth Fault Detection during Fast power Swings for Distance Protection", IEEE Transaction on Power Delivery, Vol. 10 (3), pp. 1242-1248 (1995).

[4] S. Brahama, "Distance Relay with Out-of-Step Blocking Function Using Wavelet Transform", IEEE Transactions on Power Delivery, Vol. 22 (3), pp. 1360-1366 (2007).

[5] X. Lin, Y. Gao and P. Liu, "A Novel Scheme to Identify Symmetrical Faults Occurring During Power Swings", IEEE Transactions on Power Delivery, Vol. 23 (1), pp. 73-78 (2008).

[6] EMTP Reference Models for Transmission Line Testing [Online]. Available: http:www. pes-psrc.org.

[7] Alternative Transient Program, Rule Book, Leuven EMTP Center, July (1987).

[8] A. Cavallo, R. Setola and F. Vasco, Using Matlab Simulink and Control System Toolbox, Printice Hall (1994).

[9] H. Darwish, A. Maksoud, I. Taalab and E. Ahmed, "Investigation of Power Differential Concept for line Protection," IEEE Transactions on Power Delivery, Vol. 20 (2), pp. 617-624 (2005).

Received August 25, 2008
Accepted February 23, 2009